Dear Editor and Referee,

Thanks for your suggestions which significantly help us to improve the manuscript. Hereby, we submit our responses and the manuscript has been revised accordingly. If there are any further questions or comments, please let us know.

Best regards

Renzhi Hu on behalf of all co-authors
Key Lab. of Environmental Optics & Technology, Anhui Institute of Optics and Fine Mechanics, Chinese Academy of Sciences
230031 Hefei China
E-mail: rzhu@aiofm.ac.cn

Major Comments

1. ***L 32-34: Average concentrations of OH and HO2 are provided for the LAM period in the abstract. For comparison, please also provide values for the OCM period.***

Reply:

Thanks for your suggestion. The average concentrations of OH and HO_2 are provided for the OCM period in the abstract (Line 29-33).

Revision:

Line 29-33: Under a typical ocean-atmosphere (OCM), reasonable measurement model agreement was achieved for both OH and HO_2 using a 0-D chemical box model incorporating the regional atmospheric chemistry mechanism version 2-Leuven isoprene mechanism (RACM2-LIM1), with daily averages of 4.5×10^6 cm^{-3} and 4.9×10^8 cm^{-3}, respectively.

2. ***L38-41: "After a sensitivity test, HONO-related chemistry elevated the ozone production rate by 33% and 39% during the LAM and OCM periods, respectively, while the nitric acid and sulfuric acid formation rates were 52% and 35% higher, respectively." – Please clarify the last part of this sentence. Are the nitric acid and sulfuric acid formation rate increases for the OCM or LAM period?***

Reply:

Thanks for your suggestion. The misleading sentence has been revised (line 41-44).

Revision:

Line 41-44: After a sensitivity test, HONO-related chemistry elevated the ozone production rate by 33% and 39% during the LAM and OCM periods, respectively. The nitric acid ($P(HNO_3)$) and sulfuric acid ($P(H_2SO_4)$) formation rates also increased simultaneously (~43% and ~48% for LAM and OCM sectors, respectively).

3. ***L41-43: "The simulated daytime HONO and ozone concentrations were reduced***

to a low level (~70 ppt and ~35 ppb) without the HONO constraint." – Are the reported concentrations for LAM, OCM or both periods together? For comparison, please also provide values simulated when HONO is constrained.

Reply:

Thanks for your suggestion. The modelled concentrations (~70 ppt and ~35 ppb for HONO and O_3) are the diurnal average values during the whole observation. We have added the simulated values when HONO is constrained (Line 44-46).

Revision:

Line 44-46: Without the HONO constraint, simulated O_3 decreased from ~75 ppb to a global background (~35 ppb), and daytime HONO concentration were reduced to a low level (~70 ppt).

4. ***L157-159: "A wavelength modulation for the background measurement that periodically switches from an on-resonant state to a non-resonant state has been widely used to obtain spectral zero." – Did the authors also used a chemical modulation approach as done now on most LIF-FAGE instruments to make sure that OH measurements are free from interferences? If so it should be discussed here. If not, the authors should comment on potential interferences on OH measurements.***

Reply:

Thanks for your suggestion. During the YMK campaign, we did not use a chemical modulation approach. We will discuss whether internal interference exists in AIOFM-LIF from the following aspects:

First of all, literature research shows that measurement interference is more related to the length of the inlet in the low-pressure cell (Griffith et al., 2016). In terms of system design, the AIOFM-LIF system uses a short-length inlet design to minimize this and other unknown disturbances (the distance from radical sampling to flourescence excitation is ~150 mm).

Table.S1. Comparison of key parameters related to ozonolysis reactions (O_3、alkenes、isoprene and NOx) between YMK and the intercomparison experiment. All the values are the diurnal average (10:00-15:00).

Species	Intercomparison	YMK
O_3 (ppb)	71.02	74.58
Alkenes (ppb)	1.29	1.10
Isoprene (ppb)	0.67	0.64
NOx (ppb)	5.65	4.24

Additionally, potential interference may exist when the atmosphere contains abundant alkenes, ozone, and BVOCs, indicating that environmental conditions play leading roles in OH interferences (Mao et al., 2010; Fuchs et al., 2016; Novelli et al., 2014). An OH measurement comparison with a LIF instrument deployed an inlet pre-injector (PKU-LIF), was conducted in a real atmosphere in a previous study (Zhang et al., 2022b). The ozonolysis interference on the measurement consistency of both systems was excluded under high-VOCs conditions. We have compared the chemical conditions during the intercomparison experiment and the current environmental conditions. Overall, the key parameters related to ozonolysis reactions (O_3、alkenes、isoprene and NOx) in YMK were similar to those during the comparison experiment, which is not conducive to generating potential OH interference.

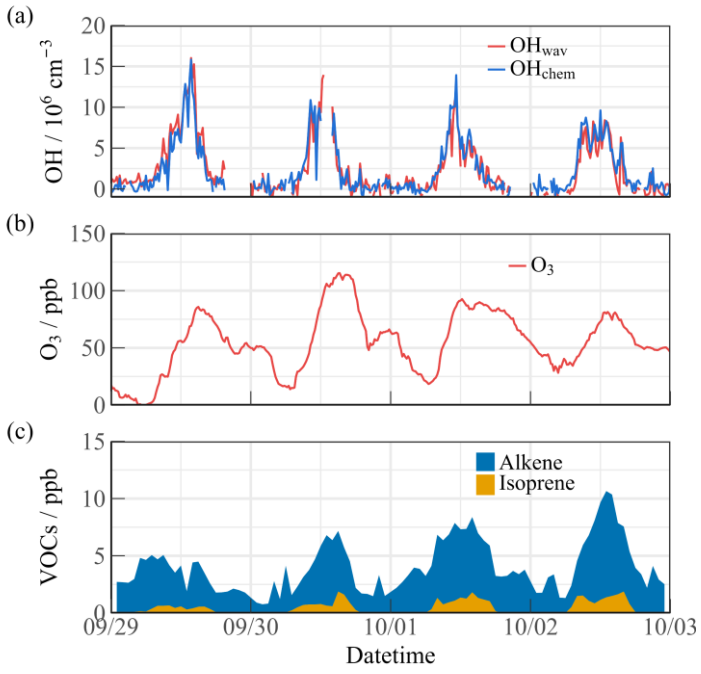

AIOFM-LIF have used a chemical modulation approach to examine the chemical

background of OH radicals in another field observation, Hefei, China. The specific description of the site is shown in (Ren et al., 2022). The environmental conditions during ozone pollution (2022.9.29-2022.10.3) are shown in the Figure above, with daytime peaks of ozone concentration above 75 ppb, accompanied by alkene species approaching ~10 ppb. The diurnal concentration of isoprene was also a high level (＞1 ppb). The chemical conditions are more favourable to induce OH interference than the YMK site (Table S1). However, the OH concentrations achieved by chemical modulation (OH_{chem}) and wavelength modulation (OH_{wav}) were in good agreement. No obvious chemical background was observed by deploying an inlet pre-injector. Therefore, it is not expected that OH measurement in the present study was affected by internal interference in the YMK site.

We added the detailed description in Line 177-187.

Revision:

Line 177-187: In terms of system design, the AIOFM-LIF system incorporates a short-length inlet design to minimize interferences from ozonolysis and other unknown factors (the distance from radical sampling to flourescence excitation is ~150 mm). An OH measurement comparison with an interference-free instrument, PKU-LIF, was conducted in a real atmosphere in a previous study (Zhang et al., 2022b). The ozonolysis interference on the measurement consistency of both systems was excluded under high-VOCs condition. Overall, the key parameters related to ozonolysis reactions (O_3、alkenes、isoprene and NOx) in YMK was similar to that during the intercomparison experiment, implies that the chemical conditions do not favor the generation of potential interference to OH measurement (Table S1).

5. "The ozone photolysis interference was subtracted according to laboratory experiments." – What was the contribution of this interference to the total measured OH signal (interference + ambient)?

Reply:

Thanks for your suggestion. We have added the Fig. S2, and the detailed

description was in Line 173-177.

Revision:

Line 173-177: Due to the synchronous reaction at 308nm, wavelength modulation is not applicable to ozone photolysis interference. Through laboratory experiments, at 20 mW laser energy, every 1% water vapor concentration and 50 ppb ozone concentration can generate a 2.5 × 10^5 cm^{-3} OH concentration. The results in this paper have subtracted the ozone photolysis interference (Fig. S2).

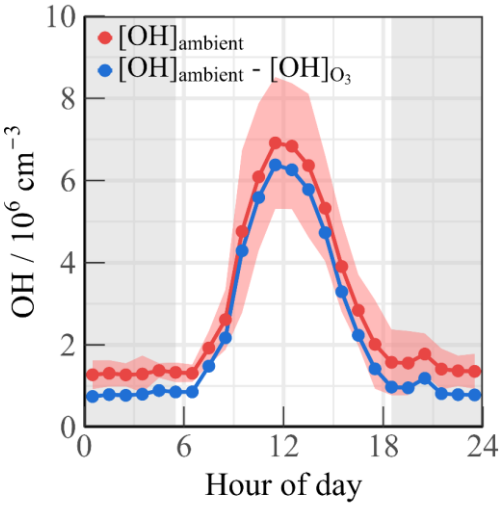

Fig. S2. Mean diurnal profiles of measured [OH] before (red line) and after (blue line) deducting the O_3 interference. The coloured shadows denote the 25 and 75% percentiles. The grey areas denote nighttime.

6. ***"The ozonolysis interference on the measurement consistency of both systems was excluded under high-NOx and high-NMHC conditions, confirming the general applicability under complex atmospheric pollution." – What do the authors mean by "ozonolysis interference"? What type of interference is it? The authors indicate that they could rule out interferences under high-NOx and high-NMHC conditions from a comparison with an interference free instrument. What about low-NOx conditions as encountered in the MBL? Why do the authors consider PKU-LIF to be free of interferences?***

Reply:

The term "ozonolysis interference" refers to a potential interference that can affect LIF-FAGE measurements of ambient OH. It is important to note that this type of interference is internally generated within the detection cell of the measurement system.

This interference arises from the ozonolysis of biogenic alkenes, as described in previous studies by Mao et al. (2012) and Rickly and Stevens (2018). The occurrence of ozonolysis interference depends on the system design and environmental conditions, particularly when the atmosphere contains significant amounts of ozone, alkenes, and BVOCs (Mao et al., 2010; Fuchs et al., 2016; Novelli et al., 2014).

The PKU-LIF system has been utilized for measuring HOx concentrations in various campaigns, and a chemical modulation approach has been employed since 2014 to quantify potential interferences (Ma et al., 2022; Yang et al., 2021; Tan et al., 2019; Tan et al., 2018a; Tan et al., 2017a). These prior studies have demonstrated that no significant internal interference existed in the PKU-LIF system, indicating that its accuracy has already been established.

In the previous comprehensive comparison experiment, AIOFM-LIF and PKU-LIF were compared under multiple conditions, including high NOx, high VOCs, low NOx, and high BVOCs. The results showed that changes in environmental conditions did not affect the measurement consistency between the two systems. Considering the key parameters related to ozonolysis reactions (O_3、alkenes、isoprene and NOx) in YMK was similar to that during the intercomparison experiment, we determined that the chemical conditions do not favor the generation of potential interference to OH measurements (Table S1).

7. ***L164-167: "For HO2 measurement, the NO concentration corresponding to a conversion efficiency of ~15% was selected to avoid RO2→HO2 interference (especially from RO2 radicals derived from long chain alkanes (C ≥ 3), alkenes, and aromatic hydrocarbons." – The authors optimized operating conditions to minimize this interference. However, to this reviewer's knowledge, it is not possible to completely eliminate this interference. The authors should comment on the level of interference that is still expected from the most abundant RO2 radicals at the measurement site. If a significant interference is expected, the authors should report this measurement as HO2* and should compare it to***

modelled HO2* values instead of HO2.

Reply:

Thank you for your response. We acknowledge and agree with the reviewer's perspective that it is challenging to completely eliminate the interference caused by RO_2 conversion. In the previous work, we have calculated the conversion efficiency of alkene-derived RO_2 to OH under different NO concentration (Wang et al., 2021). In this observation, ethene accounted for about 70% of the total ethene concentration (Table S5). Therefore, we choose ethene and isoprene to investigate the percentage interference from an alkene-derived RO_2. When NO was at 1.6×10^{12} cm^{-3}, the conversion efficiency of HO_2 was ~15%, and the percentage interference from ethene and isoprene-derived RO_2 was 3.83% and 1.75%, respectively (Wang et al., 2021). We added the detailed description in Line 187-195.

Revision:

Line 187-195: For HO_2 measurement, the NO gas was mixed with 2% in N_2 to achieve HO_2-to-OH conversion. NO was passed through a ferrous sulfate filter to remove impurities (NO_2, HONO, and so on) before being injected into the detection cell. The NO concentration (~1.6×10^{12} cm^{-3}) corresponding to a conversion efficiency of ~15% was selected to avoid $RO_2 \rightarrow HO_2$ interference (especially from RO_2 radicals derived from long-chain alkanes ($C \geq 3$), alkenes, and aromatic hydrocarbons). Previous study denoted that the percentage interference from alkene-derived RO_2 under these operating conditions was no more than 5% (Wang et al., 2021).

8. L175: "measurement errors were 13% and 17%" – Please clarify in the text how these values were assessed? If these values are derived from uncertainties associated to the generated radical concentrations it should read "measurement accuracy"

Reply:

Thanks for your suggestion. We acknowledge and agree with the reviewer's perspective that the "measurement errors" should be changed as "measurement

accuracy". We determine the value by considering the system uncertainty and calibration uncertainty, and the measurement accuracy for OH and HO_2 were 13% and 17%, respectively. We added the detailed description in Line 213-216.

Revision:

Line 213-216: Considering the system uncertainty and calibration uncertainty, the detection limits of the OH and HO_2 radicals were 3.3×10^5 cm^{-3} and 1.1×10^6 cm^{-3} (60 s, 1σ), respectively. At a typical laser power of 15 mW, the measurement accuracy for OH and HO_2 measurement was 13% and 17%, respectively.

9. L185-191: The authors should provide more details on the measured VOCs in the supplementary material. What were the most abundant species in each category (alkanes, alkenes, aromatics, OVOCs)? What was the campaign averaged concentration of each category? Etc.

Reply:

Thanks for your suggestion. The detailed information for VOCs species during the YMK campaign has been added in the Supplement (Table. S5). We added the detailed description in Line 338-339.

Revision:

Line 338-339: The detailed information for VOCs species during the YMK campaign has been added in the Table S5.

Table. S5. The detailed information table for VOCs species during the YMK campaign. The mean concentration, standard deviation (SD), minimum value (Min), maximum value (Max), and percentage contribution in the species for the top-five ranked species in alkanes, alkenes, aromatic and OVOCs are listed. All the values are the daily average (0:00-24:00).

Species	Mean (ppb)	Sd (ppb)	Min (ppb)	Max (ppb)	Proportion (%)
Alkane					
ethane	1.72	0.564	0.24	5.621	29.2
propane	1.246	0.524	0.136	5.438	21.15
n-butane	0.646	0.395	0.054	2.424	10.97
i-butane	0.561	0.471	0.029	3.372	9.52
n-hexane	0.41	0.307	0.033	3.026	6.96
Alkene					
ethene	0.592	0.656	0.034	5.48	69.08
propene	0.123	0.127	0.017	1.187	14.35

1-butene	0.046	0.014	0.012	0.107	5.37
trans-2-butene	0.028	0.006	0.006	0.05	3.27
cis-2-butene	0.026	0.006	0.007	0.045	3.03
Aromatic					
toluene	0.523	0.361	0.035	2.82	38.34
benzene	0.286	0.112	0.032	0.742	20.97
m-xylene	0.123	0.237	0.015	3.579	9.02
ethyl benzene	0.107	0.134	0.017	2.052	7.84
o-xylene	0.103	0.214	0.015	3.294	7.55
OVOC					
acetone	3.297	0.835	0.412	5.978	52.47
acetaldehyde	1.742	0.635	0.276	5.805	27.73
methyl ethyl ketone	0.496	0.15	0.051	1.118	7.89
methyl t-butyl ether	0.213	0.208	0.018	1.512	3.39
propionaldehyde	0.178	0.081	0.028	0.572	2.83

10. L191: "All of the instruments were located close to the roof of the fourth floor" – It was not indicated in the text before that there is a building at the measurement site. Please provide some details in the site description section.

Reply:

Thanks for your suggestion. The site is a part of Shenzhen ecological monitoring Center station, approximately 35 m above sea level, and the sea is approximately 150 m to the east. All of the instruments were located close to the roof of the monitoring building. We added the detailed description in Line 117-119&240-242.

Revision:

Line 118-120: The site is a part of Shenzhen Ecological Monitoring Center station, approximately 35 m above sea level, and the sea is approximately 150 m to the east.

Line 240-242: All of the instruments were located close to the roof of the monitoring building, nearly 12 m above the ground to ensure that all of the pollutants were located in a homogeneous air mass.

11. L202-204: "The overall average during the observations was substituted for large areas of missing data due to instrument maintenance or failure." – How long were these time periods? They should be highlighted in Figure 3. It is interesting

to note that while using campaign average data when ancillary measurements are missing could lead to improper model constraint, it does not appear to have a significant impact on the model-measurement agreement.

Reply:

Thanks for your suggestion. Considering the instrument failure of GC-MS in 10.24-10.26, we use the overall average data to fill the missing VOCs data. We have identified the time interval of the missing data in Fig. S3.

Revision:

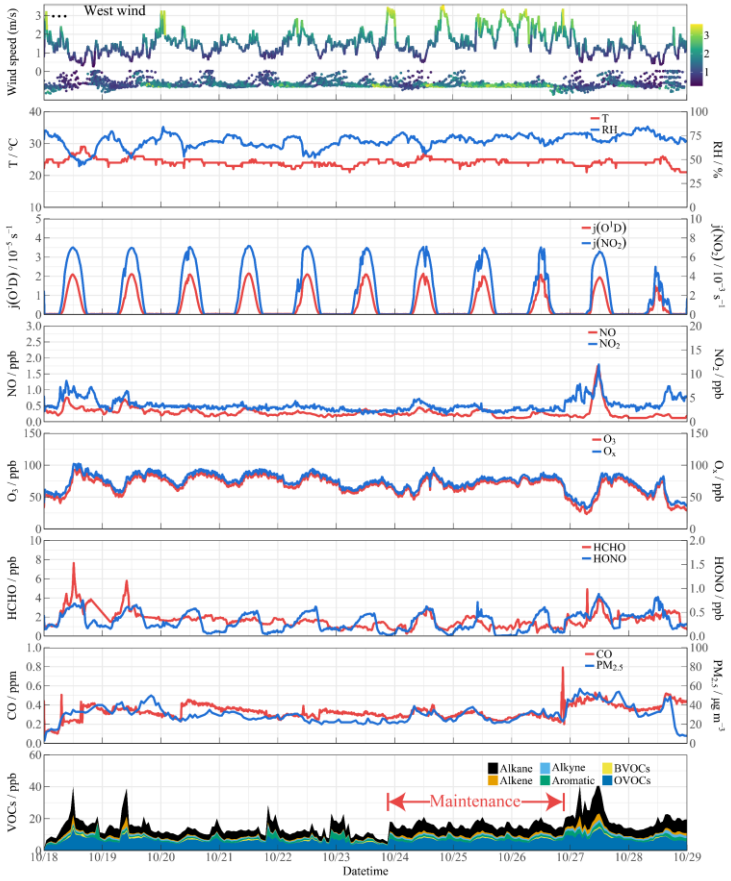

Fig. S3. Time series of observed meteorological and chemical parameters at YMK from18 October to October 28, 2019. The GC-MS instrument failed between 24 and 26 October, and the missing VOCs data were replaced by the average value during the observation period. Only isoprene was considered in the BVOCs contribution.

12. L210: "the simulation accuracy of the model for the OH and HO2 radicals was 50%" – Please specify if this is 1 or 2 σ

Reply:

Thanks for your suggestion. The simulation accuracy of the model for the OH and HO_2 radicals was 50%, 1σ.

13. L211-217: The bromine chemistry is included in the chemical mechanism to test the HOx sensitivity. What about the iodine chemistry? Is there a specific reason why it was not included in the mechanism as well?

Reply:

In response to the reviewer's suggestion, Iodine-related mechanisms are also considered in the latest version of the manuscript. In order to better explore the effect of Br and I chemistry on HOx radicals, we chose BrO/IO as the initiation point of halogen chemistry. The concentration of BrO and IO is set to ~5 ppt, which is a typical level in MBL site (Xia et al., 2022; Bloss et al., 2010; Whalley et al., 2010).

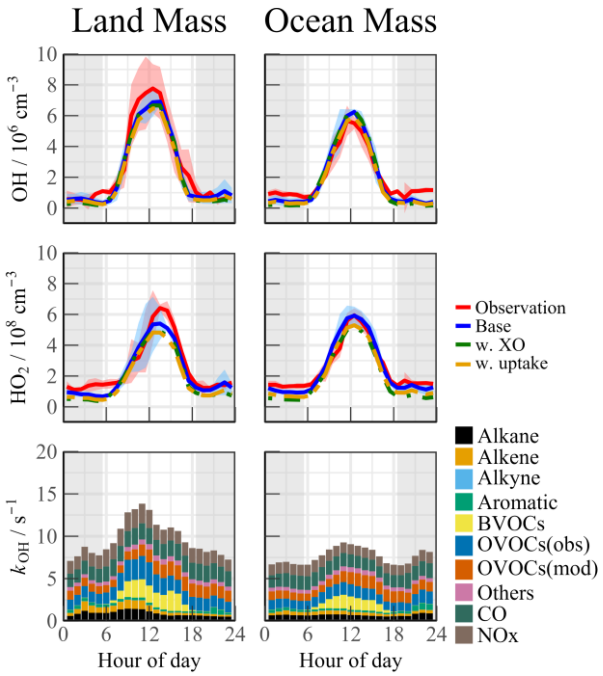

Fig. 4. Median diurnal profiles of the observed and modelled OH, HO_2, k_{OH} during LAM and OCM episodes. The coloured shadows for OH and HO_2 radicals denote the 25 and 75% percentiles. The grey areas denote nighttime.

In this scenario (Fig. 4, green line). The daytime concentration of HO_2 radical decreased by 8.5% and 13.3% during the LAM and OCM periods, respectively, compared to the base model. However, there was no significant change in the concentration of OH radicals (<3%). We added the detailed description in Line 270-276&417-426.

Revision:

Line 270-276: Considering the environmental characteristics of the MBL, the gas-phase mechanisms for bromine (Br) and iodine (I) were introduced into the base model to diagnose the impacts of the reactive bromine chemistry. The details of the mechanisms involved are listed in Tables S3 and S4. The halogen species were not available in the YMK site, so the typical levels of BrO and IO concentration in MBL site was used as a reference value (average daytime concentration of ~5 ppt) (Xia et al., 2022; Bloss et al., 2010; Whalley et al., 2010).

Line 417-426: Halogen species have been recognized as potent oxidizers that can boost photochemistry (Xia et al., 2022; Peng et al., 2021). A sensitivity test was performed by imposing BrO and IO into the base model to diagnose the impact of the halogen chemistry on the troposphere chemistry. The concentration of BrO and IO is set to ~5 ppt, which is a typical level in MBL site (Xia et al., 2022; Bloss et al., 2010; Whalley et al., 2010). The details of the mechanisms involved are listed in Tables S3 and S4. In this scenario (Fig. 4, green line). The daytime concentration of HO_2 radical decreased by 8.5% and 13.3% during the LAM and OCM periods, respectively, compared to the base model. However, there was no significant change in the concentration of OH radicals (<3%).

14. L301-302 & Fig. 3: How does the modelled kOH compare to that calculated from the model constrains? How much OH reactivity does the model generate from unconstrained OVOCs? Since VOCs are constrained as lumped groups in RACM, OH reactivity from unmeasured OVOCs may be underestimated. Could the authors comment on this?

Reply:

In response to the reviewer's suggestion, we have adopted a classification for the k_{OVOCs}, separating them into $k_{OVOCs(Obs)}$ and $k_{OVOCs(Model)}$. Specifically, $k_{OVOCs(Obs)}$ includes the observed species such as formaldehyde (HCHO), acetaldehyde (ACD), higher aldehydes (ALD), acetone (ACT), ketones (KET), and oxidation products of isoprene (MACR and MVK). The model-generated intermediates, such as glyoxal,

methylglyoxal, methylethyl ketone, and methanol, are categorized as $k_{OVOCs(Model)}$. Approximately 50% of the total k_{OVOCs} are represented by unconstrained species ($k_{OVOCs(Model)}$), which contribute a daily k_{OH} of 1.39 s^{-1}. It should be noted that the OH reactivity of unmeasured VOCs may be underestimated due to the lumped groups in RACM. We have updated Fig.4 to include this classification of k_{OVOCs}. We added the detailed description in Line 362-375.

Revision:

Line 362-375: The k_{OVOCs} was separated into $k_{OVOCs(Obs)}$ and $k_{OVOCs(Model)}$ (Fig. 3(c)). Specifically, $k_{OVOCs(Obs)}$ includes the observed species such as formaldehyde (HCHO), acetaldehyde (ACD), higher aldehydes (ALD), acetone (ACT), ketones (KET), and oxidation products of isoprene (MACR and MVK). The model-generated intermediates, such as glyoxal, methylglyoxal, methylethyl ketone, and methanol, are categorized as $k_{OVOCs(Model)}$. Approximately 50% of the total k_{OVOCs} are represented by unconstrained species ($k_{OVOCs(Model)}$), which contribute a daily k_{OH} of 1.39 s^{-1}. Overall, the observed OH and HO_2 concentrations were both well reproduced by the base model incorporating the RACM2-LIM1 mechanism. The observed OH was underestimated only on the first days, and a slight model overestimation happened on October 23&24. PSS calculation showed good agreement with the base model, providing evidence of the balance of radical internal consistency in the daytime. It should be noted that the OH reactivity of unmeasured VOCs may be underestimated due to the lumped groups in RACM2 mechanism.

15. L311-313: "The base model slightly overestimated the OH radical, suggesting that a radical removal pathway was missing." – The authors should this statement. The measurement/model agreement is well within uncertainty. In addition, this is only observed on the first 2 days and a model underestimation is observed on 10/23 & 10/24.

Reply:

Thanks for your suggestion. We have removed the statement (Line 369-372).

Revision:

Line 369-372: Overall, the observed OH and HO_2 concentrations were both well reproduced by the base model incorporating the RACM2-LIM1 mechanism. The observed OH was underestimated only on the first days, and a slight model overestimation happened on October 23&24.

16. L314-327: Model sensitivity to halogen chemistry - What was the range of BrO concentrations simulated by the model? Is it comparable to BrO concentrations measured in the MBL? As mentioned in a previous comment, iodine chemistry was not added in the model. Why? Could the authors comment on the potential impact of this chemistry?

Reply:

Thanks for your suggestion. In the previous manuscript, when the model was run with Br_2 chemistry, the diurnal concentration of BrO was depicted in the following Figure. During the observation period, BrO concentration exhibited a clear diurnal variation with peak concentrations at 0.68 ppt. This value is consistent with the simulated results observed by HZ (~0.5 ppt) but lower than those obtained at CHABLIS (~5.0 ppt) (Bloss et al., 2010; Xia et al., 2022).

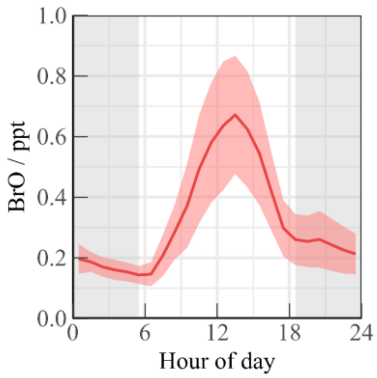

In response to the reviewer's suggestion, Iodine-related mechanisms are also considered in the latest version of the manuscript. In order to better explore the effect of Br and I chemistry on HOx radicals, we chose BrO/IO as the initiation point of halogen chemistry. The concentration of BrO and IO is set to ~5 ppt, which is a typical level in MBL site (Xia et al., 2022; Bloss et al., 2010; Whalley et al., 2010).

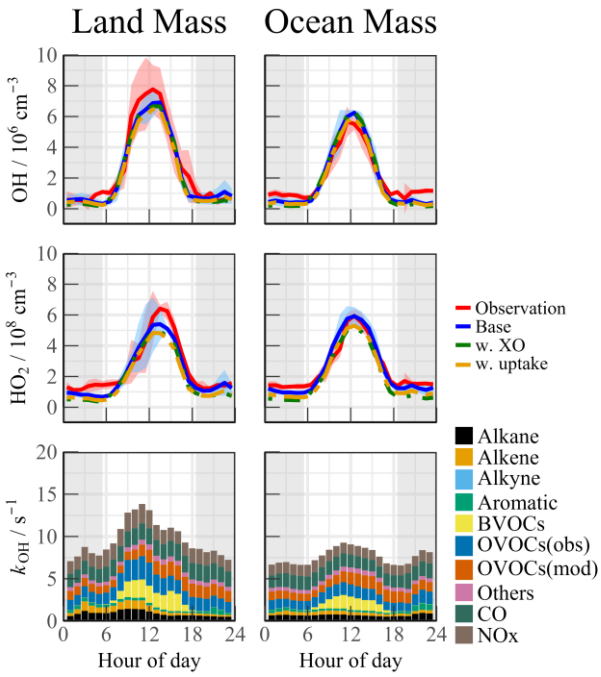

Fig. 4. Median diurnal profiles of the observed and modelled OH, HO_2, k_{OH} during LAM and OCM episodes. The coloured shadows for OH and HO_2 radicals denote the 25 and 75% percentiles. The grey areas denote nighttime.

In this scenario (Fig. 4, green line). The daytime concentration of HO_2 radical decreased by 8.5% and 13.3% during the LAM and OCM periods, respectively, compared to the base model. However, there was no significant change in the concentration of OH radicals (<3%). We added the detailed description in Line 417-426.

Revision:

Line 417-426: Halogen species have been recognized as potent oxidizers that can boost photochemistry (Xia et al., 2022; Peng et al., 2021). A sensitivity test was performed by imposing BrO and IO into the base model to diagnose the impact of the halogen chemistry on the troposphere chemistry. The concentration of BrO and IO is set to ~5 ppt, which is a typical level in MBL site (Xia et al., 2022; Bloss et al., 2010; Whalley et al., 2010). The details of the mechanisms involved are listed in Tables S3 and S4. In this scenario (Fig. 4, green line). The daytime concentration of HO_2 radical decreased by 8.5% and 13.3% during the LAM and OCM periods, respectively, compared to the base model. However, there was no significant change in the concentration of OH radicals (<3%).

17. L331-346 & Fig. 5: This reviewer does not see the added value of this section and thinks that it moves the reader's focus away from the main results. It is suggested to remove it.

Reply:

Thanks for your suggestion. The case and the previous Fig.5 have been removed to make the paper more succinct.

18. Eq. 3: The second term on the right-hand side should include the organic nitrate yield from RO2+NO. The authors may need to recalculate P(Ox) values displayed in Fig. 9 if the organic nitrate yield was not considered.

Reply:

Thanks for your suggestion. When calculating P(Ox) in the previous Fig.9, the contribution from the formation of organic nitrates has been subtracted. This portion of the side reaction process is denoted in the previous Eq.3. We added the detailed description in Line 527-528.

Revision:

Line 522, Eq.8:

$$F(O_x) = k_{HO_2+NO}[NO][HO_2] + \sum_i (1-\alpha_i) k_{RO_2^i+NO}[NO]RO_2^i \quad (8)$$

Line 527-528: α_i represents the side generation ratio of organic nitrate, which also affects the quantum yield of NO_2 (Tan et al., 2018b).

19. L529-542: Please provide details on the time dependent box model in the supplementary material.

Reply:

Thanks for your suggestion. The details on the time dependent box model have been added to the supplementary material (Text S1).

Revision:

S1 Brief overview of the ozone-prediction mode in box model

A 0-D chemical box model incorporating a condensed mechanism, the regional atmospheric chemistry mechanism version 2-Leuven isoprene mechanism (RACM2-LIM1), was used to predict ozone concentration (Stockwell et al., 1997; Griffith et al., 2013; Tan et al., 2017b). In the ozone-estimation mode, the meteorological parameters, pollutants, and precursor concentrations mentioned in Section 2.2.2 were input into the model as boundary conditions, and the temporal resolution for all of the constraints was unified to 15 min. Three days of data were entered in advance as the spin-up period. The hydrogen (H_2) and methane (CH_4) concentrations were set to fixed values of 550 ppb and 1900 ppb, respectively. The physical losses of species due to processes such as deposition, convection, and advection were approximately replaced by an 18 h atmospheric lifetime, corresponding to a first-order loss rate of ~1.5 cm/s. Constraints of the observed ozone and NO concentrations were removed on the basis of the base scenario. According to the measurement accuracy, the simulation accuracy of the model for the OH and HO_2 radicals was 50% (Zhang et al., 2022a). To specifically quantify the contribution of HONO-induced ozone generation, a sensitivity test was conducted without constraints on HONO (i.e., w.o HONO). Only the homogeneous reaction (OH + NO) participated in the formation of HONO in the default mode without HONO input.

Minor Comments

1. ***L183: "carbonic oxide" should read "carbon monoxide"***

Reply:

Thanks for your suggestion. We have revised the manuscript as the reviewer's comment (Line 223).

2. ***L271: "Serval observation campaign" should read "Several observation campaigns"***

Reply:

Thanks for your suggestion. We have revised the manuscript as the reviewer's comment.

3. ***L299: Since a range of concentrations is given for both OH and HO2, "The average daily maximum" should read "The daily maximum". Other instances in the text.***

Reply:

Thanks for your suggestion. We have revised the manuscript as the reviewer's comment in Line 26&339&356&626.

4. ***L332: Please define ROx***

Reply:

Thanks for your suggestion. We have revised the manuscript as the reviewer's comment in Line 400.

5. ***2: Please define the different parameters***

Reply:

Thanks for your suggestion. We have revised the manuscript as the reviewer's comment in Line 463-464.

Revision:

Line 463-464: Here, φ_{OH} and φ_{OH}^{i} represent the OH yields in the O_3 photolysis and alkene ozonolysis processes, respectively.

6. ***L447-448: "As the only known gas-phase source, OH + NO accounted for a negligible proportion of the HONO loss." Should read "As the only known gas-phase source, OH + NO accounted for a negligible proportion of the HONO production rate."***

Reply:

Thanks for your suggestion. We have revised the manuscript as the reviewer's comment in Line 512-513.

7. ***L455: "Peroxyl radical" should read "Peroxy radical". Other instances in the text.***

Reply:

Thanks for your suggestion. We have revised the manuscript as the reviewer's comment.

8. ***L573: "peroxynitrite" should read "peroxynitrate"***

Reply:

Thanks for your suggestion. We have revised the manuscript as the reviewer's comment in Line 504&643.

9. ***Fig S2: Please indicate the color code for back-trajectories***

Reply:

Thanks for your suggestion. We have revised the manuscript as the reviewer's comment.

Revision:

Fig. S1.: The 24-h backward trajectories calculated at an arrival time of 12:00 (local time) at 100 m (red line), 500 (blue line), 1000 m (green line) above ground level at YMK in special days;

References

Bloss, W. J., Camredon, M., Lee, J. D., Heard, D. E., Plane, J. M. C., Saiz-Lopez, A., Bauguitte, S. J. B., Salmon, R. A., and Jones, A. E.: Coupling of HOx, NOx and halogen chemistry in the antarctic boundary layer, Atmos Chem Phys, 10, 10187-10209, 10.5194/acp-10-10187-2010, 2010.

Fuchs, H., Tan, Z., Hofzumahaus, A., Broch, S., Dorn, H.-P., Holland, F., Kuenstler, C., Gomm, S., Rohrer, F., Schrade, S., Tillmann, R., and Wahner, A.: Investigation of potential interferences in the detection of atmospheric ROx radicals by laser-induced fluorescence under dark conditions, Atmos Meas Tech, 9, 1431-1447, 10.5194/amt-9-1431-2016, 2016.

Griffith, S. M., Hansen, R. F., Dusanter, S., Stevens, P. S., Alaghmand, M., Bertman, S. B., Carroll, M. A., Erickson, M., Galloway, M., Grossberg, N., Hottle, J., Hou, J., Jobson, B. T., Kammrath, A., Keutsch, F. N., Lefer, B. L., Mielke, L. H., O'Brien, A., Shepson, P. B., Thurlow, M., Wallace, W., Zhang, N., and Zhou, X. L.: OH and HO2 radical chemistry during PROPHET 2008 and CABINEX 2009-Part 1: Measurements and model comparison, Atmos Chem Phys, 13, 5403-5423, 10.5194/acp-13-5403-2013, 2013.

Griffith, S. M., Hansen, R. F., Dusanter, S., Michoud, V., Gilman, J. B., Kuster, W. C., Veres, P. R., Graus, M., de Gouw, J. A., Roberts, J., Young, C., Washenfelder, R., Brown, S. S., Thalman, R., Waxman, E., Volkamer, R., Tsai, C., Stutz, J., Flynn, J. H., Grossberg, N., Lefer, B., Alvarez, S. L., Rappenglueck, B., Mielke, L. H., Osthoff, H. D., and Stevens, P. S.: Measurements of hydroxyl and hydroperoxy radicals during CalNex-LA: Model comparisons and radical budgets, J Geophys Res-Atmos, 121, 4211-4232, 10.1002/2015jd024358, 2016.

Ma, X., Tan, Z., Lu, K., Yang, X., Chen, X., Wang, H., Chen, S., Fang, X., Li, S., Li, X., Liu, J., Liu, Y., Lou, S., Qiu, W., Wang, H., Zeng, L., and Zhang, Y.: OH and HO2 radical chemistry at a suburban site during the EXPLORE-YRD campaign in 2018, Atmos Chem Phys, 22, 7005-7028, 10.5194/acp-22-7005-2022, 2022.

Mao, J., Ren, X., Chen, S., Brune, W. H., Chen, Z., Martinez, M., Harder, H., Lefer, B., Rappenglück, B., Flynn, J., and Leuchner, M.: Atmospheric oxidation capacity in the summer of Houston 2006: Comparison with summer measurements in other metropolitan studies, Atmos Environ, 44, 4107-4115, 10.1016/j.atmosenv.2009.01.013, 2010.

Novelli, A., Hens, K., Ernest, C. T., Kubistin, D., Regelin, E., Elste, T., Plass-Duelmer, C., Martinez, M., Lelieveld, J., and Harder, H.: Characterisation of an inlet pre-injector laser-induced fluorescence instrument for the measurement of atmospheric hydroxyl radicals, Atmos Meas Tech, 7, 3413-3430, 10.5194/amt-7-3413-2014, 2014.

Peng, X., Wang, W. H., Xia, M., Chen, H., Ravishankara, A. R., Li, Q. Y., Saiz-Lopez, A., Liu, P. F., Zhang, F., Zhang, C. L., Xue, L. K., Wang, X. F., George, C., Wang, J. H., Mu, Y. J., Chen, J. M., and Wang, T.: An unexpected large continental source of reactive bromine and chlorine with significant impact on wintertime air quality, Natl. Sci. Rev., 8, 10.1093/nsr/nwaa304, 2021.

Ren, B., Xie, P. H., Xu, J., Li, A., Qin, M., Hu, R. Z., Zhang, T. S., Fan, G. Q., Tian, X., Zhu, W., Hu, Z. K., Huang, Y. Y., Li, X. M., Meng, F. H., Zhang, G. X., Tong, J. Z., Ren, H. M., Zheng, J. Y., Zhang, Z. D., and Lv, Y. S.: Vertical characteristics of NO2 and HCHO, and the ozone formation regimes in Hefei, China, Sci Total Environ, 823, 10.1016/j.scitotenv.2022.153425, 2022.

Stockwell, W. R., Kirchner, F., Kuhn, M., and Seefeld, S.: A new mechanism for regional atmospheric chemistry modeling, J Geophys Res-Atmos, 102, 25847-25879, 10.1029/97jd00849, 1997.

Tan, Z., Fuchs, H., Lu, K., Hofzumahaus, A., Bohn, B., Broch, S., Dong, H., Gomm, S., Haeseler, R., He, L., Holland, F., Li, X., Liu, Y., Lu, S., Rohrer, F., Shao, M., Wang, B., Wang, M., Wu, Y., Zeng, L., Zhang, Y., Wahner, A., and Zhang, Y.: Radical chemistry at a rural site (Wangdu) in the North China Plain: observation and model calculations of OH, HO2 and RO2 radicals, Atmos Chem Phys, 17, 663-690, 10.5194/acp-17-663-2017, 2017a.

Tan, Z., Rohrer, F., Lu, K., Ma, X., Bohn, B., Broch, S., Dong, H., Fuchs, H., Gkatzelis, G. I., Hofzumahaus, A., Holland, F., Li, X., Liu, Y., Liu, Y., Novelli, A., Shao, M., Wang, H., Wu, Y., Zeng, L., Hu, M., Kiendler-Scharr, A., Wahner, A., and Zhang, Y.: Wintertime photochemistry in Beijing: observations of ROx radical concentrations in the North China Plain during the BEST-ONE campaign, Atmos Chem Phys, 18, 12391-12411, 10.5194/acp-18-12391-2018, 2018a.

Tan, Z. F., Lu, K. D., Dong, H. B., Hu, M., Li, X., Liu, Y. H., Lu, S. H., Shao, M., Su, R., Wang, H. C., Wu, Y. S., Wahner, A., and Zhang, Y. H.: Explicit diagnosis of the local ozone production rate and the ozone-NOx-VOC sensitivities, Sci. Bull., 63, 1067-1076, 10.1016/j.scib.2018.07.001, 2018b.

Tan, Z. F., Lu, K. D., Hofzumahaus, A., Fuchs, H., Bohn, B., Holland, F., Liu, Y. H., Rohrer, F., Shao, M., Sun, K., Wu, Y. S., Zeng, L. M., Zhang, Y. S., Zou, Q., Kiendler-Scharr, A., Wahner, A., and Zhang, Y. H.: Experimental budgets of OH, HO2, and RO2 radicals and implications for ozone formation in the Pearl River Delta in China 2014, Atmos Chem Phys, 19, 7129-7150, 10.5194/acp-19-7129-2019, 2019.

Tan, Z. F., Fuchs, H., Lu, K. D., Hofzumahaus, A., Bohn, B., Broch, S., Dong, H. B., Gomm, S., Haseler, R., He, L. Y., Holland, F., Li, X., Liu, Y., Lu, S. H., Rohrer, F., Shao, M., Wang, B. L., Wang, M., Wu, Y. S., Zeng, L. M., Zhang, Y. S., Wahner, A., and Zhang, Y. H.: Radical chemistry at a rural site (Wangdu) in the North China Plain: observation and model calculations of OH, HO2 and RO2 radicals, Atmos Chem Phys, 17, 663-690, 10.5194/acp-17-663-2017, 2017b.

Wang, Y., Hu, R., Xie, P., Chen, H., Wang, F., Liu, X., Liu, J., and Liu, W.: Measurement of tropospheric HO2 radical using fluorescence assay by gas expansion with low interferences, J Environ Sci (China), 99, 40-50, 10.1016/j.jes.2020.06.010, 2021.

Whalley, L. K., Furneaux, K. L., Goddard, A., Lee, J. D., Mahajan, A., Oetjen, H., Read, K. A., Kaaden, N., Carpenter, L. J., Lewis, A. C., Plane, J. M. C., Saltzman, E. S., Wiedensohler, A., and Heard, D. E.: The chemistry of OH and HO2 radicals in the boundary layer over the tropical Atlantic Ocean, Atmos Chem Phys, 10, 1555-1576, 2010.

Xia, M., Wang, T., Wang, Z., Chen, Y., Peng, X., Huo, Y., Wang, W., Yuan, Q., Jiang, Y., Guo, H., Lau, C., Leung, K., Yu, A., and Lee, S.: Pollution-Derived Br2 Boosts Oxidation Power of the Coastal Atmosphere, Environ Sci Technol, 10.1021/acs.est.2c02434, 2022.

Yang, X., Lu, K., Ma, X., Liu, Y., Wang, H., Hu, R., Li, X., Lou, S., Chen, S., Dong, H., Wang, F., Wang, Y., Zhang, G., Li, S., Yang, S., Yang, Y., Kuang, C., Tan, Z., Chen, X., Qiu, P., Zeng, L., Xie, P., and Zhang, Y.: Observations and modeling of OH and HO2 radicals in Chengdu, China in summer 2019, The Science of the total environment, 772, 144829-144829, 10.1016/j.scitotenv.2020.144829, 2021.

Zhang, G., Hu, R., Xie, P., Lou, S., Wang, F., Wang, Y., Qin, M., Li, X., Liu, X., Wang, Y., and Liu, W.: Observation and simulation of HOx radicals in an urban area in Shanghai, China, Sci Total Environ, 810, 152275, 10.1016/j.scitotenv.2021.152275, 2022a.

Zhang, G., Hu, R., Xie, P., Lu, K., Lou, S., Liu, X., Li, X., Wang, F., Wang, Y., Yang, X., Cai, H., Wang, Y., and Liu, W.: Intercomparison of OH radical measurement in a complex atmosphere in Chengdu, China, Sci Total Environ, 155924, 10.1016/j.scitotenv.2022.155924, 2022b.